International Journal of Thermophysics, Vol. 18, No. 3, 1997

Thermophysical Properties of Aqueous NaOH–H_2O Solutions at High Concentrations

J. Olsson,[1] Å. Jernqvist,[1] and G. Aly[1,2]

Received October 10, 1996

The working fluids, used in the majority of all mechanical heat pumps, are expected to be phased out within some few years due to their contribution to the stratospheric ozone depletion and global warming. Absorption heat pumps and transformers are receiving a new renaissance in the field of heating, refrigeration, air-conditioning, and heat recovery. Sodium hydroxide solutions are more propitious to the pulp and paper industry compared to other working pairs. Novel correlations have been developed to compute the vapor pressure, density, enthalpy, and viscosity of sodium hydroxide solutions. These correlations cover the most extensive range of validity ever proposed: 273–473 K for temperatures and 0.2–1 kg water per kg solution for concentrations.

KEY WORDS: absorption; density; enthalpy; heat pump; sodium hydroxide; vapor pressure; viscosity.

1. INTRODUCTION

Absorption heat pumps (AHPs) and transformers (AHTs) are currently used in the field of refrigeration, air-conditioning, heating, and heat recovery. A well known reason for the renaissance of absorption technology is the impact on the ozone layer by chlorofluorinated carbons (CFCs) and/or hydrochlorofluorinated carbons (HCFCs), used in the majority of all mechanical heat pumps, and their contribution to the greenhouse effect. These agents are expected to be phased out within some few years. Some of the many working fluids that have been proposed for use in industrial AHPs and AHTs include H_2O–LiBr, H_2O–NaOH, NH_3–H_2O, H_2O–H_2SO_4, CH_3OH–LiBr, waters–glycerol, water–glycol, water–nitrate

[1] Department of Chemical Engineering 1, University of Lund, P.O. Box 124, S-22100 Lund, Sweden.

[2] To whom correspondence should be addressed.

0195-928X/97/0500-0779$12.50/0

salts, NH_3–inorganic salt complexes, and water–zeolites. A number of potential industrial applications have recently been suggested by Jernqvist and co-workers [1–6], who showed clearly that sodium hydroxide solutions are more propitious to the pulp and paper industry compared to other working pairs.

For proper engineering design of different components involved in these systems, reliable information is needed concerning physical and thermodynamic properties of the working fluids. A database for a number of these working fluids has been compiled [2]. The literature survey in this study revealed a serious lack in the physical and thermodynamic properties of sodium hydroxide solutions within the ranges of temperature and concentration that are interesting in the industrial applications of absorption heat pumps and transformers. The databases which were searched are Chemical Abstracts, Compendex, and Energy.

In this work, we present correlations yielding highly accurate data for the vapor pressure, enthalpy, density, and viscosity of sodium hydroxide solutions within temperature and concentration ranges of 0–200°C and 0.2–1 kg water per kg solution, respectively.

2. VAPOR PRESSURE

Table I summarizes the experimentally available information on the vapor pressure (also known as the bubble-point pressure) of $NaOH/H_2O$ solutions. Most of these data are reported for rather limited ranges of temperature, pressure, and/or concentration. Some of these studies [7–13] have also reported a vapor–pressure correlation which is based exclusively on the corresponding measurements and hence, these correlations imply a

Table I. Literature Sources of Experimental Data for Vapor Pressure

First author	Ref. No.	Year	Temp. range (°C)	Conc. range (kg H_2O/kg soln)	No. data points
Balej	7	1985	0–300	0.500–0.926	179
Campbell	8	1984	150–250	0.870–0.987	45
Hayward	9	1930	30–80	0.338–1.000	53
Int. Critical Tables	10	1928	0–350	0.012–1.000	222
Krey	11	1972	0–350	0.2–0.9	230
Krumgal'z	12	1964	150–400	0.1–0.7	135
Akerlöf	13	1940	0–70	0.595–1.000	144

limited range of applicability to engineering design of each of these correlations. The sets of data, reported in these publications, were used in this work to develop a new correlation that covers a wider range of temperature and concentration. The data were first crosschecked with each other to ensure a good accuracy of the derived correlation. For instance, all available vapor pressure data at 60 and 200°C are plotted in Fig. 1, where it can be observed that data given in International Critical Tables [10] diverge from the other data sets and were consequently not used in this work.

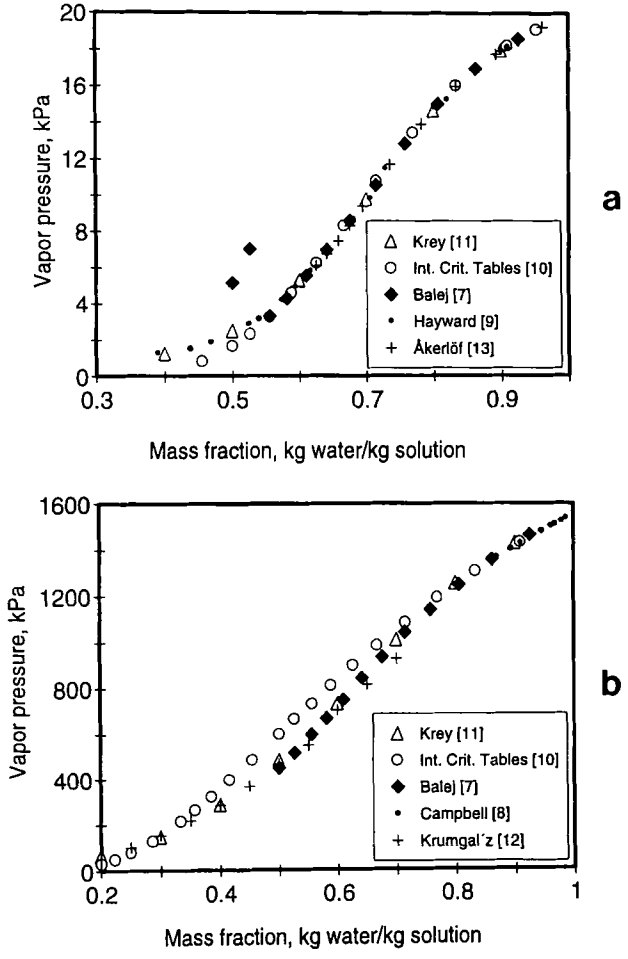

Fig. 1. Literature vapor pressure data at two temperatures: (a) 60°C; (b) 200°C.

The correlation for vapor pressure is based on the well-known Antoine equation (1), which is widely used to correlate boiling point and vapor pressure for pure liquids over a limited temperature range. In this work, it was assumed that the relationship between bubble point and vapor pressure for a solution at constant concentration of a nonvolatile solute, such as the binary $NaOH/H_2O$ solution, can be described by Antoine equation. This assumption is based on the fact that the normal melting and boiling-point temperatures of pure NaOH are 322 and 1557°C, respectively, and hence its vapor pressure at the temperature interval investigated in this study is practically small enough to be neglected. The constants a, b, and c below should correspondingly be specified for the concentration to which they are correlated.

$$\ln P = a + \frac{b}{c + t} \tag{1}$$

Equation (1) is transformed to a linear expression, as given by Eq. (2), between the logarithmic value of vapor pressure P and solution temperature t.

$$a_1 + a_2 t + a_3 \ln P = t \ln P \tag{2}$$

In a binary system, the coefficients in Eq. (2) become functions of the concentration, and it is therefore important to determine accurate correlations between the coefficients a_1, a_2, and a_3 and mass fraction x (kg H_2O · kg^{-1} soln). A number of polynomial functions were tested and it was found that Eqs. (3)–(5) result in sufficiently accurate correlations.

$$a_1 = k_{P0} + k_{P1} \ln x + k_{P2}(\ln x)^2 + \cdots + k_{P8}(\ln x)^8 \tag{3}$$

$$a_2 = l_{P0} + l_{P1} \ln x + l_{P2}(\ln x)^2 + \cdots + l_{P10}(\ln x)^{10} \tag{4}$$

$$a_3 = m_{P0} + m_{P1} \ln x + m_{P2}(\ln x)^2 + \cdots + m_{P10}(\ln x)^{10} \tag{5}$$

The higher degrees of these polynomial functions were found to be necessary to ensure a high accuracy of the entire correlation. The numerical values of the constants k_{Pi}, l_{Pj}, and m_{Pj} in Eqs. (3)–(5) are given in Table II.

The advantage of using Antoine equation is that it can be used directly to calculate either the vapor pressure P or the bubble point t. On the other hand, an iterative procedure is required to calculate the mass fraction x at a given bubble point.

Table II. Numerical Values of the Constants in Eqs. (3)–(5)

k_{P0}	−113.93947	l_{P0}	16.240074	m_{P0}	−226.80157
k_{P1}	209.82305	l_{P1}	−11.864008	m_{P1}	293.17155
k_{P2}	494.77153	l_{P2}	−223.47305	m_{P2}	5081.8791
k_{P3}	6860.8330	l_{P3}	−1650.3997	m_{P3}	36752.126
k_{P4}	2676.6433	l_{P4}	−5997.3118	m_{P4}	131262.00
k_{P5}	−21740.328	l_{P5}	−12318.744	m_{P5}	259399.54
k_{P6}	−34750.872	l_{P6}	−15303.153	m_{P6}	301696.22
k_{P7}	−20122.157	l_{P7}	−11707.480	m_{P7}	208617.90
k_{P8}	−4102.9890	l_{P8}	−5364.9554	m_{P8}	81774.024
		l_{P9}	−1338.5412	m_{P9}	15648.526
		l_{P10}	−137.96889	m_{P10}	906.29769

Table III. Temperature and Concentration Ranges for Vapor Pressure and Density Correlations

Vapor-pressure correlation, Eqs. (2)–(5)		Density correlation, Eqs. (6)–(9)	
Temp. range (°C)	Conc. range (kg H_2O/kg soln)	Temp. range (°C)	Conc. range (kg H_2O/kg soln)
$0 \leqslant t < 20$	$0.582 \leqslant x \leqslant 1$	$0 \leqslant t < 10$	$0.800 \leqslant x \leqslant 1$
$20 \leqslant t < 60$	$0.500 \leqslant x \leqslant 1$	$10 \leqslant t < 20$	$0.700 \leqslant x \leqslant 1$
$60 \leqslant t < 70$	$0.353 \leqslant x \leqslant 1$	$20 \leqslant t < 60$	$0.500 \leqslant x \leqslant 1$
$70 \leqslant t < 150$	$0.300 \leqslant x \leqslant 1$	$60 \leqslant t < 70$	$0.400 \leqslant x \leqslant 1$
$150 \leqslant t \leqslant 200$	$0.200 \leqslant x \leqslant 1$	$70 \leqslant t < 150$	$0.300 \leqslant x \leqslant 1$
		$150 \leqslant t \leqslant 200$	$0.200 \leqslant x \leqslant 1$

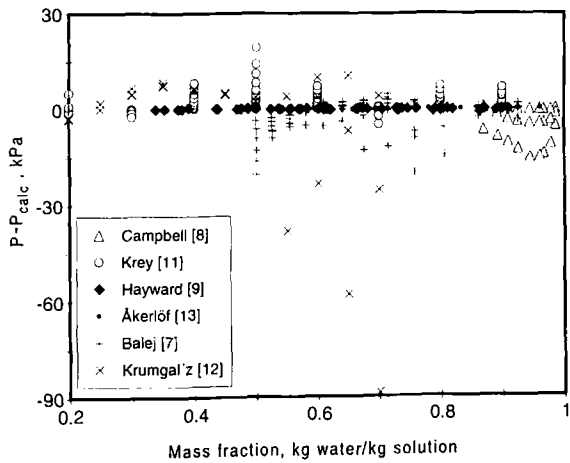

Fig. 2. Absolute deviation between experimental and computed vapor pressure data.

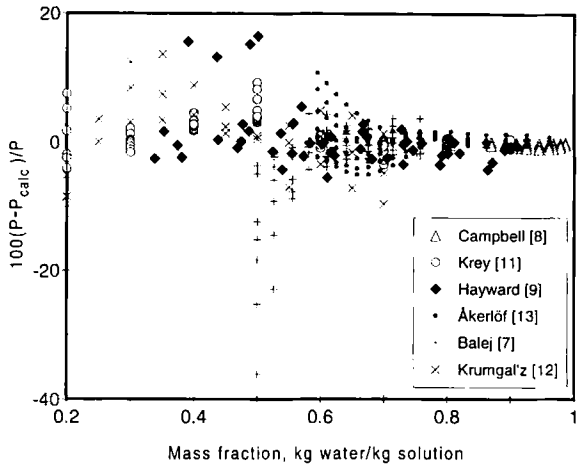

Fig. 3. Relative deviation between experimental and computed vapor pressure data.

It should be pointed out that the vapor pressure correlation, represented by Eqs. (2)–(5) above, must be used within the temperature and concentration ranges indicated in Table III, since these ranges reflect the validity of the experimental data used to derive it.

A total of 512 experimental data was used in the derivation of the vapor pressure correlation. Figure 2 depicts the absolute deviation between experimental data and computed values using the derived correlation. The corresponding values of the relative deviation are displayed in Fig. 3. The absolute and relative average errors for vapor pressure are 2.01 Kpa and 2.07%, respectively. The corresponding errors for the bubble point are 0.48 K and 0.13%, respectively. The deviation depends mostly on the discrepancies between different experimental data sets. For instance, Figs. 2 and 3 indicate that the experimental data given by Balej [7] diverge, within a certain concentration range, from the other data sets.

3. DENSITY

All experimental data, covering a temperature range between 0 and 200°C, are taken from Krey [11]. It turned out that a simple polynomial function, given by Eq. (6), is sufficiently accurate to describe the temperature dependence of the density. The coefficients b_1–b_3 are functions of the water mass fraction $x(\text{kg } H_2O \cdot \text{kg}^{-1} \text{ soln})$ and can be calculated by Eqs. (7)–(9).

Table IV. Numerical Values of the Constants in Eqs. (7)–(9)

$k_{\rho 0}$	5007.2279636	$l_{\rho 0}$	−64.786269079	$m_{\rho 0}$	0.24436776978
$k_{\rho 1}$	−25131.164248	$l_{\rho 1}$	525.34360564	$m_{\rho 1}$	−1.9737722344
$k_{\rho 2}$	74107.692582	$l_{\rho 2}$	−1608.4471903	$m_{\rho 2}$	6.04601497138
$k_{\rho 3}$	−104657.48684	$l_{\rho 3}$	2350.9753235	$m_{\rho 3}$	−8.9090614947
$k_{\rho 4}$	69821.773186	$l_{\rho 4}$	−1660.9035108	$m_{\rho 4}$	6.37146769397
$k_{\rho 5}$	−18145.911810	$l_{\rho 5}$	457.64374355	$m_{\rho 5}$	−1.7816083111

$$\rho = b_1 + b_2 t + b_3 t^2 \tag{6}$$

$$b_1 = k_{\rho 0} + k_{\rho 1} x^{1/2} + k_{\rho 2} x + k_{\rho 3} x^{3/2} + k_{\rho 4} x^2 + k_{\rho 5} x^{5/2} \tag{7}$$

$$b_2 = l_{\rho 0} + l_{\rho 1} x^{1/2} + l_{\rho 2} x + l_{\rho 3} x^{3/2} + l_{\rho 4} x^2 + l_{\rho 5} x^{5/2} \tag{8}$$

$$b_3 = m_{\rho 0} + m_{\rho 1} x^{1/2} + m_{\rho 2} x + m_{\rho 3} x^{3/2} + m_{\rho 4} x^2 + m_{\rho 5} x^{5/2} \tag{9}$$

The experimental data were used to correlate the constants in Eqs. (7)–(9) and the resulting values are given in Table IV. The above correlation, represented by Eqs. (6)–(9), is valid within the temperature and concentration ranges tabulated in Table III.

A total of 156 experimental data was used in the derivation of density correlation. Figure 4 depicts the relative deviation between experimental data and computed values using the derived correlation. The absolute and relative average errors for the solution density are 0.48 $kg \cdot m^{-3}$ and 0.04%, respectively, while the corresponding values for the maximum

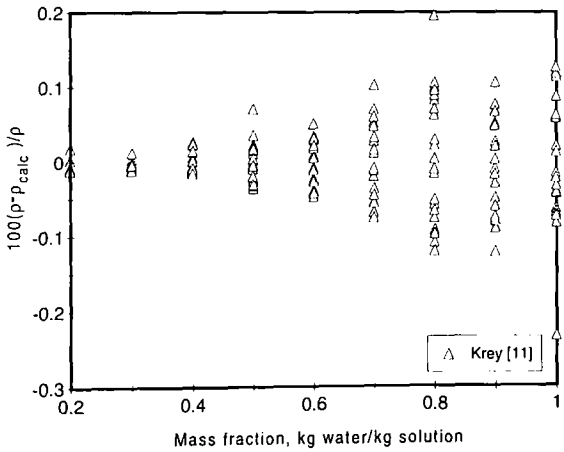

Fig. 4. Relative deviation between experimental and computed density data.

errors are 2.41 $kg \cdot m^{-3}$ and 0.23%, respectively. As can be seen, this correlation yields very small deviations. This can be explained by the fact that the surface of the density function has a rather simple structure. For instance, the smallest value of density is only twice as small as the largest value within the investigated temperature and concentration ranges. Moreover, the experimental data seem to have been measured with a high accuracy.

4. ENTHALPY

The literature survey [14–17] indicated that there is a lack of enthalpy data covering the temperature and concentration ranges investigated in this work. It was therefore necessary to find heat capacity data and use these to calculate new enthalpies within these ranges. Unfortunately, experimental heat capacity data within the intervals 100–200°C and 0.5–0.9 kg water/kg solution could not be found and were extrapolated instead, using experimental data available within other temperature and concentration ranges. The literature sources for these data are given in Table V.

It should be noted that all experimental data were recalculated to the standard states of liquid water at 0°C and an infinitely diluted sodium hydroxide solution at 20°C. Equation (10) was used to calculate new solution enthalpies from both experimental enthalpy data covering the whole concentration range at 20°C [15] and heat capacity data [16–18] within the concentration range 0.5–1 kg water/kg solution.

$$\left(\frac{\partial H}{\partial T}\right)_{P,x} = Cp(T) \tag{10}$$

Table V. Literature Sources of Experimental Data for Enthalpy (H) and Specific Heat (Cp)

First author	Ref. No.	Year	Temp. range (°C)	Conc. range (kg H_2O/kg soln)	No. data points
Wilson (H)	14	1942	27–204	0.22–0.5	427
Bertetti (H)	15	1936	20	0.52–0.98	24
Bertetti (Cp)	16	1936	0–93	0.48–1.00	264
Ackermann (Cp)	17	1957	10–130	0.926–0.980	27
Wilson (Cp)	14	1942	27–149	0.22–0.5	146

All enthalpy values were calculated at atmospheric pressure. Equation (11) can be used to recalculate the enthalpy at other pressures. However, the pressure dependence was found to be negligible.

$$\left(\frac{\partial H}{\partial T}\right)_{T,x} = \frac{1}{\rho} - T\left(\frac{\partial(1/\rho)}{\partial T}\right)_{P} \tag{11}$$

The polynomial function, given by Eq. (12), can be used to correlate the solution enthalpy, H, as a nonlinear function of temperature, t. This functional form has also been used by Feuerecker et al. [19] to correlate the enthalpy for $LiBr/H_2O$ solutions.

$$H = c_1 + c_2 t + c_3 t^2 + c_4 t^3 \tag{12}$$

The coefficients c_1–c_4 are polynomial functions of mass fraction x(kg H_2O · kg $^{-1}$ soln) and are expressed by Eqs. (13)–(16). It should be noted that the first coefficient c_1 gives the solution enthalpy at 0°C.

$$c_1 = \frac{k_{II0} + k_{II2}x + k_{II4}x^2 + k_{II6}x^3}{1 + k_{II1}x + k_{II3}x^2 + k_{II5}x^3 + k_{II7}x^4} \tag{13}$$

$$c_2 = l_{II0} + l_{II1}x + \cdots + l_{II8}x^8 \tag{14}$$

$$c_3 = m_{II0} + m_{II1}x + \cdots + m_{II7}x^7 \tag{15}$$

$$c_4 = n_{II0} + n_{II1}x + \cdots + n_{II7}x^7 \tag{16}$$

The numerical values of the constants in Eqs. (13)–(16) are given in Table VI. It should be noted that the enthalpy correlation, represented by Eqs. (12)–(16), must be used within the temperature and concentration ranges indicated in Table VII.

Table VI. Numerical Values of the Constants in Eqs. (13)–(16)

k_{II0}	1288.4485	l_{II0}	2.3087919	m_{II0}	0.02302860	n_{II0}	−8.5131313E−5
k_{II1}	−0.49649131	l_{II1}	−9.0004252	m_{II1}	−0.37866056	n_{II1}	136.52823E−5
k_{II2}	−4387.8908	l_{II2}	167.59914	m_{II2}	2.4529593	n_{II2}	−875.68741E−5
k_{II3}	−4.0915144	l_{II3}	−1051.6368	m_{II3}	−8.2693542	n_{II3}	2920.0398E−5
k_{II4}	4938.2298	l_{II4}	3394.3378	m_{II4}	15.728833	n_{II4}	−5488.2983E−5
k_{II5}	7.2887292	l_{II5}	−6115.0986	m_{II5}	−16.944427	n_{II5}	5841.8034E−5
k_{II6}	−1841.1890	l_{II6}	6220.8249	m_{II6}	9.6254192	n_{II6}	−3278.7483E−5
k_{II7}	−3.0202651	l_{II7}	−3348.8098	m_{II7}	−2.2410628	n_{II7}	754.45993E−5
		l_{II8}	743.87432				

Table VII. Temperature and Concentration Ranges for Enthalpy and Viscosity Correlations

Enthalpy correlation, Eqs. (12)–(16)		Viscosity correlation, Eqs. (17)–(21)	
Temp. range (°C)	Conc. range (kg H_2O/kg soln)	Temp. range (°C)	Conc. range (kg H_2O/kg soln)
$0 \leq t < 4$	$0.780 \leq x \leq 1$	$20 \leq t < 30$	$0.60 \leq x \leq 1$
$4 \leq t < 10$	$0.680 \leq x \leq 1$	$30 \leq t < 50$	$0.55 \leq x \leq 1$
$10 \leq t < 15$	$0.580 \leq x \leq 1$	$50 \leq t < 70$	$0.45 \leq x \leq 1$
$15 \leq t < 26$	$0.540 \leq x \leq 1$	$70 \leq t < 150$	$0.30 \leq x \leq 1$
$26 \leq t < 37$	$0.440 \leq x \leq 1$	$150 \leq t \leq 200$	$0.20 \leq x \leq 1$
$37 \leq t < 48$	$0.400 \leq x \leq 1$		
$48 \leq t < 60$	$0.340 \leq x \leq 1$		
$60 \leq t < 71$	$0.300 \leq x \leq 1$		
$71 \leq t < 82$	$0.280 \leq x \leq 1$		
$82 \leq t < 93$	$0.240 \leq x \leq 1$		
$93 \leq t \leq 204$	$0.220 \leq x \leq 1$		

A total of 901 experimental and extrapolated data was used in the derivation of the enthalpy correlation. Figure 5 shows a plot of the correlation where the calculated and extrapolated areas are indicated. The relative deviation between experimental/extrapolated data and computed values is displayed in Fig. 6. The absolute and relative average errors for the

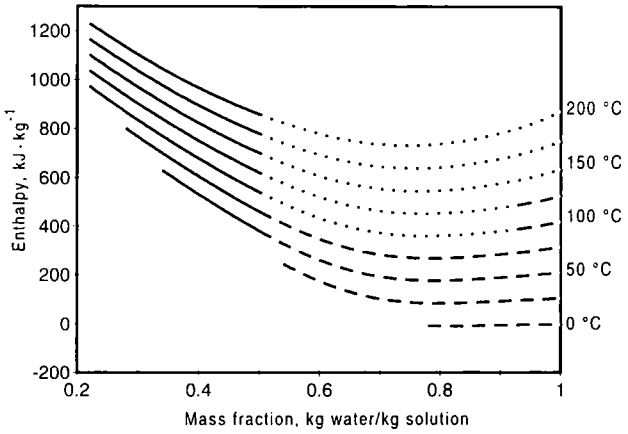

Fig. 5. Plot of the enthalpy correlation. (——) Computed using experimental enthalpy data; (--------) computed using extrapolated specific heat data; (– – – –) computed using experimental specific heat data.

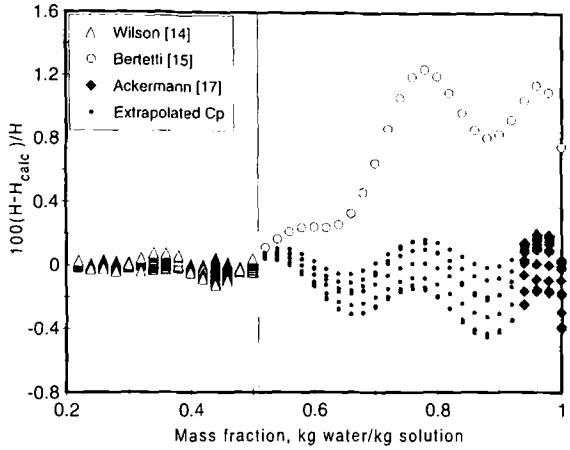

Fig. 6. Relative deviation between experimental and computed enthalpy data.

solution enthalpy are 0.32 kJ · kg^{-1} and 0.08%, respectively, while the corresponding values for the maximum errors are 2.15 kJ · kg^{-1} and 1.24%, respectively. It should be noted that experimental enthalpy data were used within the concentration range 0.20–0.52 kg H_2O kg^{-1} soln, while experimental data for the specific heat of aqueous sodium hydroxide solutions were used to compute the enthalpy at concentrations above 0.52 kg H_2O · kg^{-1} soln. The vertical line in Fig. 6 was plotted to indicate this difference.

5. VISCOSITY

The literature survey resulted in three publications [20–22], presented in Table VIII, that contain some experimental data for viscosity. Unfortunately, data at low water concentrations and high temperatures are missing. Moreover, very few viscosity data could be found in literature at high water concentrations and low temperatures (0–20°C). For instance, the experimental results of Mashovets et al. [20] include only four viscosity data within this range. Since considerable changes are expected in the viscosity of aqueous sodium hydroxide solutions within the temperature range 0–20°C, it was decided not to include these four data and to restrict the correlation to temperatures above 20°C. Existing data were therefore used to extrapolate new data points. To facilitate the extrapolation and the subsequent derivation of an appropriate viscosity correlation, the term $\ln(\mu_{solution}/\mu_{water})_T$ was calculated for each data point. This calculation

Table VIII. Literature Sources of Experimental Data for Viscosity

First author	Ref. No.	Year	Temp. range (°C)	Conc. range (kg H_2O/kg soln)	No. data points
Mashovets	20	1970	0–275	0.556–0.980	52
Baron	21	1967	25–90	0.520–1.000	30
Krings	22	1948	22–70	0.272–1.000	69

results in a more appropriate structure of the functional surface which is conditional for a good correlation.

Equation (18) was used to correlate the viscosity, μ, of the sodium hydroxide solution as a function of temperature t. Equations (17)–(20) were used to calculate the coefficients d_1–d_3 as polynomial functions of mass fraction x(kg H_2O kg^{-1} soln).

$$\ln\left(\frac{\eta_{\text{solution}}}{\eta_{\text{water}}}\right)_T = d_1 + d_2 t^{0.5} + d_3 t \tag{17}$$

$$d_1 = k_{\mu 1}(1-x) + \cdots + k_{\mu 4}(1-x)^4 \tag{18}$$

$$d_2 = l_{\mu 1}(1-x) + \cdots + l_{\mu 5}(1-x)^5 \tag{19}$$

$$d_3 = m_{\mu 1}(1-x) + \cdots + m_{\mu 5}(1-x)^5 \tag{20}$$

The data tabulated in Ref. 18 were used to derive Eq. (21) for the viscosity of pure water.

$$\eta_{\text{water}} = \exp(n_{\mu 0} + n_{\mu 1} t + n_{\mu 2} t^{1.5} + n_{\mu 3} t^{2.5} + n_{\mu 4} t^3) \tag{21}$$

The numerical values of the constants k, l, m, and n in Eqs. (18)–(21), respectively, are tabulated in Table IX. The viscosity correlation, given by Eqs. (17)–(21), is valid within the temperature and concentration ranges indicated in Table VII.

Table IX. Numerical Values of the Constants in Eqs. (18)–(21)

$k_{\mu 1}$	−6.1420727	$l_{\mu 1}$	2.3171396	$m_{\mu 1}$	−0.1152143	$n_{\mu 0}$	0.5868156
$k_{\mu 2}$	124.64849	$l_{\mu 2}$	−23.153644	$m_{\mu 2}$	1.0543467	$n_{\mu 1}$	−0.0398182
$k_{\mu 3}$	−247.08170	$l_{\mu 3}$	49.267937	$m_{\mu 3}$	−2.3693277	$n_{\mu 2}$	0.00247793
$k_{\mu 4}$	147.73585	$l_{\mu 4}$	−36.970260	$m_{\mu 4}$	2.0099091	$n_{\mu 3}$	−4.9427*E−6
		$l_{\mu 5}$	6.5882887	$m_{\mu 5}$	−0.5257284	$n_{\mu 4}$	1.48701*E−7

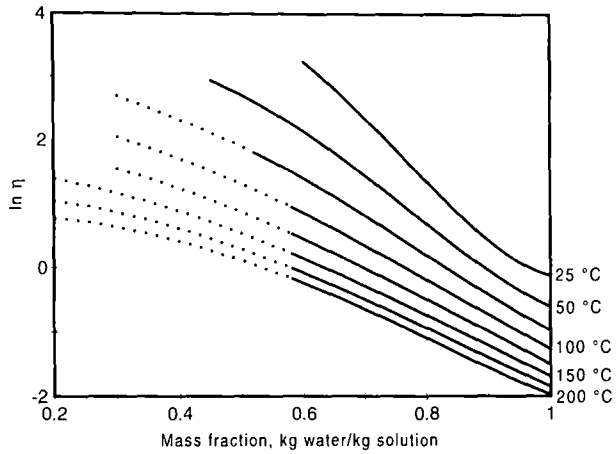

Fig. 7. Plot of the viscosity correlation. (——) Computed using experimental viscosity data; (--------) computed using extrapolated data.

The solution viscosity is plotted as function of mass fraction in Fig. 7, where the calculated and extrapolated areas are also indicated. The relative deviation between experimental data and computed values, using the derived correlation for the viscosity, is shown in Fig. 8. The absolute and relative average errors for the solution viscosity are 0.17 cP and 2.13%,

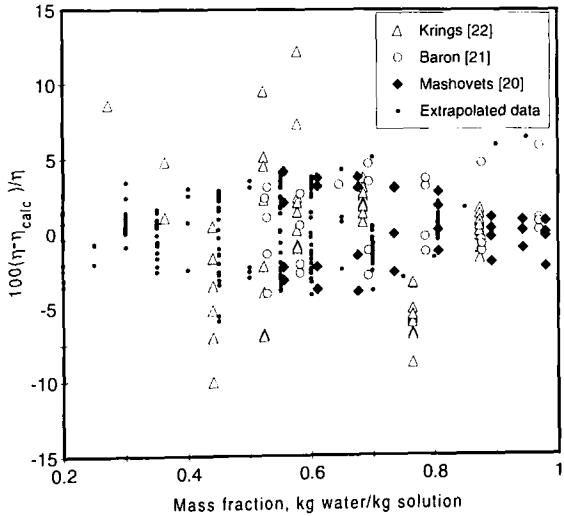

Fig. 8. Relative deviation between experimental and computed viscosity data.

respectively while the corresponding values for the maximum errors are 5.6 cP and 12.2%, respectively. As can be observed, the accuracy of this correlation is not as good as the correlations derived in this work for the other physical properties. The lack of experimental data in some intervals of the temperature and concentration ranges should contribute to some uncertainty. Another factor could be the degree of accuracy of the available experimental data. For instance, some of the data reported by Krings [22] diverge, within the mass fraction interval 0.25–0.75, from other experimental data.

ACKNOWLEDGMENTS

The authors would like to thank Mr. A. Gränfors, H. Kockum, and G. Ternström for valuable discussions and kind help with the softwares Mathlab and Table Curve. The financial support of the Swedish National Board for Industrial and Technical Development is gratefully acknowledged.

NOMENCLATURE

a_i Coefficients in Eq. (2)
b_i Coefficients in Eq. (6)
c_i Coefficients in Eq. (12)
Cp Specific heat ($kJ \cdot kg^{-1} \cdot K^{-1}$)
d_i Coefficients in Eq. (18)
H Enthalpy of solution ($kJ \cdot kg^{-1}$ soln)
k_{Pi} Constants in Eq. (3), given in Table II
$k_{\rho i}$ Constants in Eq. (7), given in Table IV
k_{Hi} Constants in Eq. (13), given in Table VI
$k_{\mu i}$ Constants in Eq. (18), given in Table IX
l_{Pi} Constants in Eq. (4), given in Table II
$l_{\rho i}$ Constants in Eq. (8), given in Table IV
l_{Hi} Constants in Eq. (14), given in Table VI
$l_{\mu i}$ Constants in Eq. (19), given in Table IX
m_{Pi} Constants in Eq. (5), given in Table II
$m_{\rho i}$ Constants in Eq. (9), given in Table IV
m_{Hi} Constants in Eq. (15), given in Table VI
$m_{\mu i}$ Constants in Eq. (20), given in Table IX
n_{Hi} Constants in Eq. (16), given in Table VI
$n_{\mu i}$ Constants in Eq. (21), given in Table IX
P Vapor pressure of solution (kPa)
t Temperature (°C)

x Mass fraction of $NaOH–H_2O$ solution ($kg\ H_2O \cdot kg^{-1}$ soln)
μ Dynamic viscosity [$cP(g \cdot s^{-1} \cdot m^{-1})$]
ρ Density ($kg \cdot m^{-3}$)

REFERENCES

1. K. Abrahamsson, G. Aly, and A. Jernqvist, *Nordic Pulp Paper Res. J.* **6**:9 (1992).
2. K. Abrahamsson, *Dissertation* (Dept. Chem. Eng. I, Lund University, Lund, Sweden, 1993).
3. M. Gierow and A. Jernqvist, in *Proceedings of International Absorption Heat Pump Conference*, AES-Vol. 31 (1994), p. 303.
4. K. Abrahamsson, G. Aly, A. Jernqvist, and S. Stenström, in *Proceedings of International Absorption Heat Pump Conference*, AES-Vol. 31 (1994), p. 295.
5. A. Gidner, A. Jernqvist, and G. Aly, *Appl. Therm. Eng.* **16**:33 (1996).
6. K. Abrahamsson, S. Stenström, G. Aly, and A. Jernqvist, *Int. J. Energy Res.* (1997), to appear.
7. J. Balej, *Int. J. Hydrogen Energy* **10**:233 (1985).
8. A. N. Campbell and O. N. Bhatnager, *J. Chem. Eng. Data* **29**:166 (1984).
9. A. M. Hayward and E. P. Perman, *Trans. Faraday Soc.* **23**:95 (1927).
10. E. Washburn (ed.), *International Critical Tables of Numerical Data, Physics, Chemistry and Technology, Vol. 3* (McGraw-Hill, New York, 1928), p. 373.
11. J. Krey, *Z. phys. Chem. Neue Folge* **81**:252 (1972).
12. B. S. Krumgal'z and V. P. Mashovets, *Zh. Prikl. Khim.* (Leningrad) **37**:2750 (1964).
13. G. Akerlöf and G. Kegeles, *J. Am. Chem. Soc.* **62**:620 (1940).
14. H. R. Wilson and W. L. McCabe, *Ind. Eng. Chem.* **34**:558 (1942).
15. J. W. Bertetti and W. L. McCabe, *Ind. Eng. Chem.* **28**:247 (1936).
16. J. W. Bertetti and W. L. McCabe, *Ind. Eng. Chem.* **28**:375 (1936).
17. T. Ackermann, *Discuss. Faraday Soc.* **24**:180 (1957).
18. *VDI-Wärmeatlas*, 7th ed., Db1-Db15 (VDI-Verlag, Düsseldorf, 1994).
19. G. Feuerecker, J. Scharfe, I. Greiter, C. Frank, and G. Alefeld, in *Proceedings of International Absorption Heat Pump Conference*, AES-Vol. 31 (1994), p. 493.
20. V. P. Mashovets, L. V. Puchkov, P. M. Sargaev, and M. K. Fedorov, *Zh. Prikl. Khim.* (Leningrad) **46**:992 (1973).
21. N. M. Baron and R. P. Matveeva, *J. Appl. Chem. USSR* **40**:652 (1967).
22. V. W. Krings, *Z. Anorganische Chem.* **255**:294 (1948).